Acta of Bioengineering and Biomechanics
Vol. 21, No. 1, 2019

Original paper
DOI: 10.5277/ABB-01274-2018-02

Influence of middle ear disorder in round-window stimulation using a finite element human ear model

KAI ZHOU[1], HOUGUANG LIU[1*], JIANHUA YANG[1], YU ZHAO[1], ZHUSHI RAO[2], SHANGUO YANG[1]

[1] School of Mechatronic Engineering, China University of Mining and Technology, Xuzhou, P. R. China.
[2] State Key Laboratory of Mechanical System and Vibrations, Shanghai Jiao Tong University, Shanghai, P. R. China.

Purpose: The aim of this work was to study the effect of middle ear disorder on round window (RW) stimulation, so as to provide references for the optimal design of RW stimulation type middle ear implants (MEIs). *Methods*: A human ear finite-element model was built by reverse engineering technique based on micro-computed tomography scanning images of human temporal bone, and was validated by three sets of comparisons with experimental data. Then, based on this model, typical disorders in otosclerosis and otitis media were simulated. Finally, their influences on the RW stimulation were analyzed by comparison of the displacements of the basilar membrane. *Results*: For the otosclerosis, the stapedial abnormal bone growth severely deteriorated the equivalent sound pressure of the RW stimulation at higher frequencies, while the hardening of ligaments and tendons prominently decreased the RW stimulation at lower frequencies. Besides, among the hardening of the studied tissues, the influence of the stapedial annular ligament's hardening was much more significant. For the otitis media, the round window membrane (RWM)'s thickening mainly decreased the RW stimulation's performance at lower frequencies. When the elastic modulus' reduction of the RWM was considered at the same time especially for the acute otitis media, it would raise the lower-frequency performance of the RW stimulation. *Conclusions*: The influence of the middle ear disorder on the RW stimulation is considerable and variable, it should be considered during the design of the RW stimulation type MEIs.

Key words: *middle ear implant, round-window stimulation, otosclerosis, otitis media, hearing loss, finite-element analysis*

1. Introduction

The situation of hearing loss is becoming more and more serious in the society. The World Health Organization notes that there are nearly 360 million people worldwide suffering from varying degrees of hearing impairment. Based on the location of dysfunction, hearing impairments are divided into two types: sensorineural and conductive. With the development of otology, conductive hearing loss can be improved by drugs or surgeries. For the patients with sensorineural hearing loss, the best choice is still the traditional hearing aid as there is no effective treatment for them. Unfortunately, there are some inherent defects in hearing aids, such as ringing, occlusion of the ear canal, limited amplification, and cosmetic appearance. To solve this problem, different kinds of middle ear implants (MEIs) have been proposed and developed [16]. Unlike hearing aids that compensate hearing loss based on their loudspeakers' acoustical stimulation to the eardrum, MEIs commonly use their implanted actuators to stimulate the ossicles to work, which is called forward drive. However, some patients suffer from middle ear disorders such as otosclerosis and otitis media (OM), which makes it difficult to couple the actuator to an ossicle. To address this issue, reverse drive or round window (RW) stimulation, which stimulates the round window membrane (RWM) by coupling the actuator to the inner ear, was proposed and developed.

Despite encouraging clinical outcomes of the RW stimulation, there is still a large uncertainty in its hear-

* Corresponding author: Houguang Liu, School of Mechatronic Engineering, China University of Mining and Technology, Da Xue Road No. 1, Xuzhou, 221116, P.R. China. Phone: +8618761435299, e-mail: liuhg@cumt.edu.cn
Received: December 15th, 2018
Accepted for publication: January 9th, 2019

ing compensation performance. In order to find out the cause of this variability, a number of researches have been performed. Arnold et al. [2] indicated that placing the actuator perpendicularly to the RWM could get better implant performance than in tight fixation condition, and covering the actuator with connective tissue would be more beneficial. Koka et al. [14] also found that coupling the actuator with RWM by soft tissue could enhance the acoustic energy transferring to the cochlea. Maier et al. [18] further demonstrated that the static preloading applied to the actuator would cause the diversity of MEIs' performance. Considering the finite-element (FE) method shows a distinct advantage in simulating the tiny and complex ear system, Zhang et al. [28] constructed a three-dimensional FE model of the human ear, so as to investigate the effect of MEIs' parameters on RW stimulation by changing the size and weight of the actuator. Their results showed that smaller actuator size could make the RW stimulation's capacity better. Further, Tian et al. [25] reported that introducing a middle layer between the RWM and the actuator could reduce the actuator's size requirements. In addition, Liu et al.'s numerical results [17] proved that the higher the elastic modulus of the middle layer set, the worse the performance of RW stimulation. All these studies have made outstanding contributions in the improvement of RW stimulation's performance, but they are only concerning on the design parameters of the actuator.

Since the RW stimulation is mainly used to treat hearing loss with the coexistence of otosclerosis or OM [5], the patient-specific variables associated with these middle ear disorders may also influence the capability of the RW stimulation. To investigate the influence of the RWM's lesion, Yao et al. [27] constructed a mechanical model of RWM. Their model-predicted RWM's responses showed that both the shrinkage of the RWM (caused by otosclerosis) and the thickening (caused by the OM) would reduce the RWM's displacement excited by RW stimulation. Gan et al. [23] found that the RWM's thickening would coincide with its elastic modulus decease in acute otitis media (AOM). Besides, the effect of the ossicular chain lesions in otosclerosis, such as the fixation of the malleus, and the stapedial abnormal bone growth, also need to be investigated.

Accordingly, in this paper, to study the effect of otosclerosis and OM on round-window stimulation, we constructed and verified a human ear FE model by reverse engineering technique based on micro-computed tomography (Micro-CT). Then, based on this model, typical disorders associated with the otosclerosis and OM were simulated. By comparing the basilar membrane (BM) displacements at the frequency-dependent characteristic positions, the effects of these disorders on the RW stimulation performance were studied comparatively. The results are intended to insure the adequate compensation and support the optimal design of the RW stimulation type MEI.

2. Materials and methods

2.1. Human ear finite element model

In this study, first we established a human ear FE model incorporating the middle ear and the cochlea. The model mainly based on our previously established human ear FE model [25]. According to a fresh temporal bone of a 45-year-old male's right ear, the middle ear section's geometric model was established by the technology of Micro-CT and reverse engineering [3], [6]. Then using Hypermesh, a FE pre-processing software, to generate its corresponding FE model which consists of the tympanic membrane, ossicles (i.e., the stapes, incus, and malleus), suspensory ligaments, and tendons. A total of 804 three-noded shell elements were created to mesh the eardrum and tympanic annulus ligament. The other parts of the middle ear were meshed by 48043 four-noded tetrahedral elements. The geometric model of the cochlear section was constructed manually. The structure and size of the cochlear geometric model was the same as in our previous report [25], but the difference was that the RWM's thickness of our current model was set to 70 μm [29]. The fluid in scala vestibuli and scala tympani were meshed by 17577 and 13802 eight-noded hexahedral elements. The BM was meshed by 482 four-noded shell elements. A total of 408 four-noded tetrahedral elements were created to mesh the RWM. Figure 1 shows the final constructed human ear FE model.

Assuming that the entire middle ear portion's material properties are uniform, isotropic and elastic, with a Poisson's ratio of 0.3 [8]. Referring to the published data [8], [9], [25] and taking a cross-calibration on that, the densities and the elastic moduli of the middle ear components were ascertained and listed in Table 1. For the cochlear section, the apex of its BM elastic modulus was assumed to be 3 MPa, the middle was 15 MPa, and the base was 40 MPa [25]. The fluid's density and volume modulus in the cochlea were defined as 1000 kg/m^3 and 2250 MPa, respectively [25]. The elastic moduli of the RWM and the support of the BM were 2.32 MPa and 14100 MPa [29].

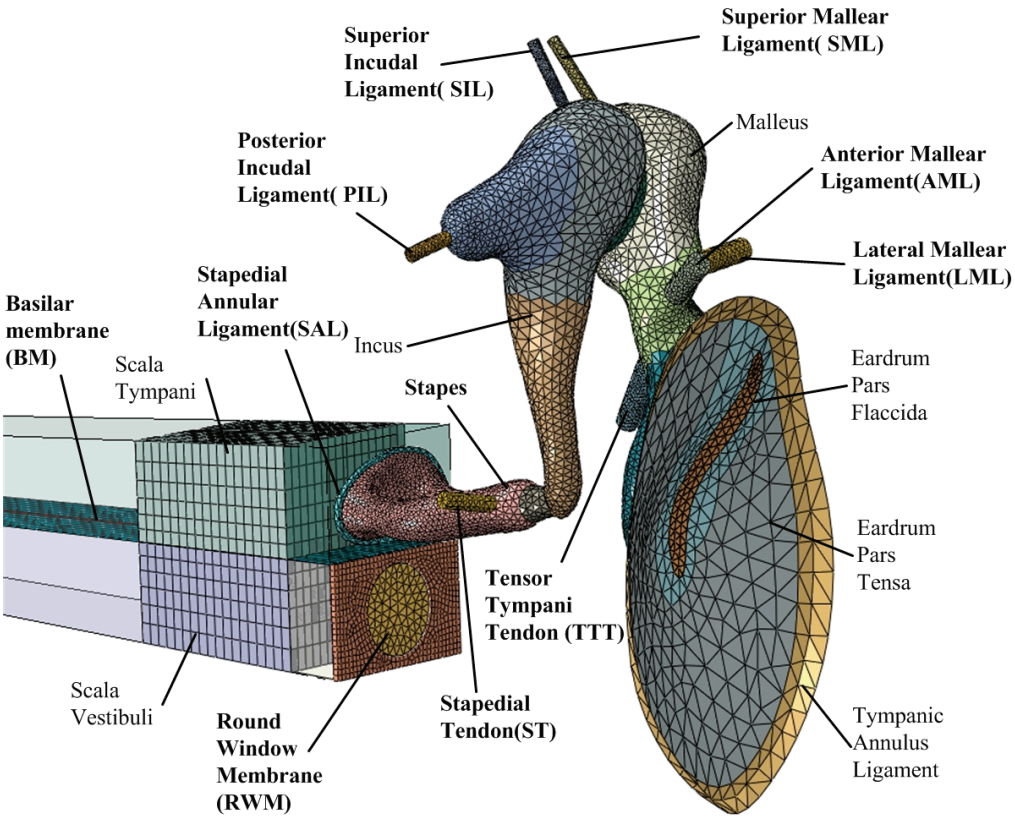

Fig. 1. The constructed FE model of the human ear

Table 1. The ascertained properties of our model's middle ear portion

Component	Our model	Published data
1	**2**	**3**
Eardrum		
Density [kg/m^3]	1.2×10^3	1.2×10^3 [25]
Young's modulus [Pa]		
Pars tensa	3×10^7	3×10^7 [25]
Pars flaccida	1×10^7	1×10^7 [25]
Malleus		
Density [kg/m^3]		
Head	2.55×10^3	2.55×10^3 [8]
Neck	4.53×10^3	4.53×10^3 [8]
Young's modulus [Pa]	1.41×10^{10}	1.41×10^{10} [8]
Manubrium		
Density [kg/m^3]	1×10^3	1×10^3 [8]
Young's modulus [Pa]	4.7×10^9	4.7×10^9 [8]
Incus		
Density [kg/m^3]		
Long process	5.08×10^3	5.08×10^3 [8]
Short process	2.26×10^3	2.26×10^3 [8]
Body	2.36×10^3	2.36×10^3 [8]
Young's modulus [Pa]	1.41×10^{10}	1.41×10^{10} [8]
Stapes		
Density [kg/m^3]	2.2×10^3	2.2×10^3 [8]
Young's modulus [Pa]	1.41×10^{10}	1.41×10^{10} [8]
Incudomalleoular joint		

1	2	3
Density [kg/m^3]	3.2×10^3	3.2×10^3 [8]
Young's modulus [Pa]	1.41×10^{10}	1.41×10^{10} [8]
Incudostapedial joint		
Density [kg/m^3]	1.2×10^3	1.2×10^3 [8]
Young's modulus [Pa]	4.4×10^5	6×10^5 [8]
Tympanic annulus ligament		
Density [kg/m^3]	1.2×10^3	1.2×10^3 [25]
Young's modulus [Pa]	1.5×10^5	3×10^5 [25]
Superior mallear ligament		
Density [kg/m^3]	2.5×10^3	2.5×10^3 [25]
Young's modulus [Pa]	4.9×10^4	4.9×10^4 [9]
Lateral mallear ligament		
Density [kg/m^3]	2.5×10^3	2.5×10^3 [25]
Young's modulus [Pa]	6.7×10^4	6.7×10^4 [9]
Posterior incudal ligament		
Density [kg/m^3]	2.5×10^3	2.5×10^3 [25]
Young's modulus [Pa]	6.5×10^7	6.5×10^7 [25]
Anterior mallear ligament		
Density [kg/m^3]	2.5×10^3	2.5×10^3 [25]
Young's modulus [Pa]	2.1×10^7	2.1×10^7 [25]
Stapedial tendon		
Density [kg/m^3]	2.5×10^3	2.5×10^3 [25]
Young's modulus [Pa]	2.6×10^7	5.2×10^7 [25]
Superior incudal ligament		
Density [kg/m^3]	2.5×10^3	1×10^3 [9]
Young's modulus [Pa]	4.9×10^6	4.9×10^4 [9]
Tensor tympani tendon		
Density [kg/m^3]	2.5×10^3	2.5×10^3 [25]
Young's modulus [Pa]	7×10^8	7×10^7 [25]
Stapedial annular ligament		
Density [kg/m^3]	1.2×10^3	1.2×10^3 [25]
Young's modulus [Pa]	1.5×10^4	1×10^4 [9]

The energy loss of human ear was simulating by setting the material properties of some soft issues including incudomalleoular joint, incudostapedial joint, eardrum pars flaccida, eardrum pars tensa, RWM and stapedial annular ligament as viscoelastic. Their relaxation moduli can be obtained by Eq. (1).

$$E(t) = E_0(1 + e_1 e^{-t/\tau_1}), \tag{1}$$

where, E_0 is the elastic modulus, t is the time, e_1 and τ_1 are the viscoelasticity parameters; they all list in Table 2 [28]. Except these soft issues, Rayleigh damping was applied to the other parts of human ear to simulate their energy loss. Specifically, $\alpha = 0$ s^{-1}, $\beta = 0.75 \times 10^{-4}$ s [8], and $\alpha = 0$ s^{-1}, $\beta = 0.75 \times 10^{-5}$ s [26], were the damping coefficients of the middle ear and BM, respectively.

To simulate the boundary condition for the FE model, the ligaments, the tendons, the RWM and the BM support were fixed; the internal fluid of the cochlea was confined in the cochlea, and the normal gradient of its pressure near the cochlear bone wall was 0 Pa/m. Besides, fluid-structure interaction was defined on the surfaces of the cochlear fluid elements that contacted with the movable tissues, i.e., the footplate of the stapes, the basilar membrane, and the round window.

Table 2. The viscoelasticity parameters of the soft tissues in our human ear FE model

Component	e_1	τ_1/μs
Incudomalleolar joint	5.99	20
Incudostapedial joint	65.67	20
Eardrum pars flaccida	4	25
Eardrum pars tensa	6	25
Round window membrane	0.43	30
Stapedial annular ligament	3.76	24

2.2. Simulation of the otosclerosis and otitis media in FE model

2.2.1. Otosclerosis

Otosclerosis can cause the damage to ossicular chain, such as the fixation of ossicles [21] and abnormal growth of the stapes [20]. To simulate the ossicles fixation, we respectively increased the elastic moduli of the corresponding ligaments and tendon: the anterior mallear ligament (AML), lateral mallear ligament (LML), superior mallear ligament (SML), tensor tympani tendon (TTT), posterior incudal ligament (PIL), superior incudal ligament (SIL), and the stapedial annular ligament (SAL). Except the SAL, the elastic moduli of other ligaments were increased by 1000 times to simulate their calcifications [13]. To simulate the SAL's change in the otosclerosis, its elastic modulus was increased by 100 times to accomplish a 30 dB sound conduction deterioration [13]. As for the abnormal growth of stapes, we increased the stapes mass by a factor of 5 to mimic this symptom [7].

2.2.2. Otitis media

Similar to Yao et al.'s study [27], we mainly focused on the effect of RWM's lesion in OM. Based on human temporal bone study, Sahni et al. [24] indicated that different types of OM caused different thickness of the RWM, such as serous otitis media (SOM), purulent otitis media (POM), chronic otitis media (COM) and acute otitis media (AOM). The approximate values of measured thicknesses for different form of OM are listed in Table 3. To simulate these types of OM, the RWM's thicknesses was changed in our FE model accordingly. Besides, in the AOM, Gan et al. [23] found that the stiffness of the RWM decreased simultaneously. Thus, the RWM's elastic modulus reduced to 12% of the original value at the same time in simulating the AOM [23].

Table 3. The RWM's thickness in different types of OM

Types	Normal	SOM	POM	COM	AOM
RWM's thickness /μm	70	89	95.6	111.4	140

2.3. Simulation of RW stimulation

The purpose of this paper was to study the effect of the middle ear disorders on RW stimulation's performance, not the effect of MEI's parameters, so the specific structure of actuator was not considered in the model. Considering the most common actuator used in RW stimulation is electromagnetic one, which is a force driven actuator, the RW stimulation was simulated by applying a driving force onto the surface of RW along the normal direction of the RW. To generate the equivalent BM response caused by a 90 dB sound pressure applied on the tympanic membrane, the magnitude of the applied force on the RWM was set to 50 μN, according to Zhang et al. [28].

2.4. Calculation of the equivalent sound pressure (ESP)

The sensation of hearing is owing to the response of the cochlear BM at the frequency-dependent characteristic position. Therefore, in order to evaluate the MEIs' performance accurately, we used the BM displacement to assess the RW stimulation performance. Specifically, the corresponding ESP of the RW stimulation can be obtained by Eq. (2)

$$P_{eq} = 90 + 20\log_{10}\left(\frac{d_{rw}}{d_{ac}}\right), \tag{2}$$

where, d_{ac} and d_{rw} are the BM displacements that were excited by a 90 dB SPL sound pressure on the tympanic membrane, and a 50 μN force on the RWM, respectively.

3. Results

3.1. Validation of the FE model

In order to ensure the reliability of the model, it was validated by comparison of three sets of data, which were calculated by 90 dB SPL sound pressure applied on the tympanic membrane.

The cochlear frequency selectivity, which acts as a spectral analyzer and decomposes sounds into constituent frequencies, is the most important property characterizing the cochlea. Specifically, the BM next to the cochlea's base is sensitive to the higher frequencies while the part next to the cochlea's apex is sensitive to the lower frequencies; different longitudinal positions on the BM are sensitive to specific frequencies. Since this property is fundamental to hearing, it was initially selected to verify the reliability of our model. As can be seen from Fig. 2, the

data obtained from our model agrees well with the experimental values of Békésy et al. [4] and Skarstein et al. [15].

In addition, the BM vibration's transfer function was calculated at a specific BM position (12 mm from the cochlear base). The results of model-predicted were plotted to compare to the experimental values obtained from Gundersen et al. [12] in Fig. 3. It shows that our model-predicted BM's relative motion amplitude and the relative motion phase are all consistent with those measured by Gundersen et al. [12] Figure 3a also shows the sensitive frequency of 12 mm on the BM along the cochlear longitudinal direction is 4000 Hz, which complies with the results in Fig. 2.

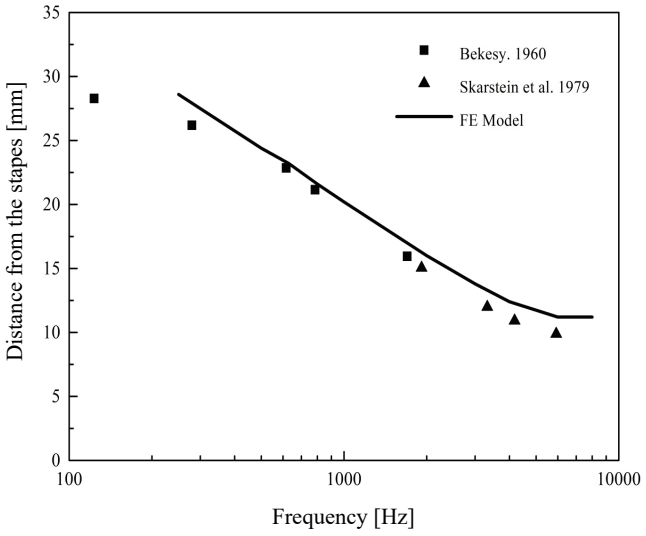

Fig. 2. Correspondence between the characteristic frequency and longitudinal position of BM

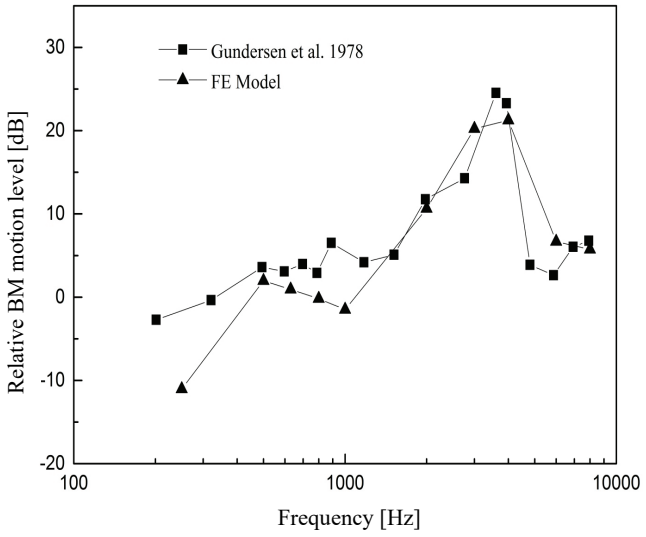

Fig. 3a. Amplitude of BM motion relative to stapes footplate motion for the human cochlea at 12 mm from the stapes

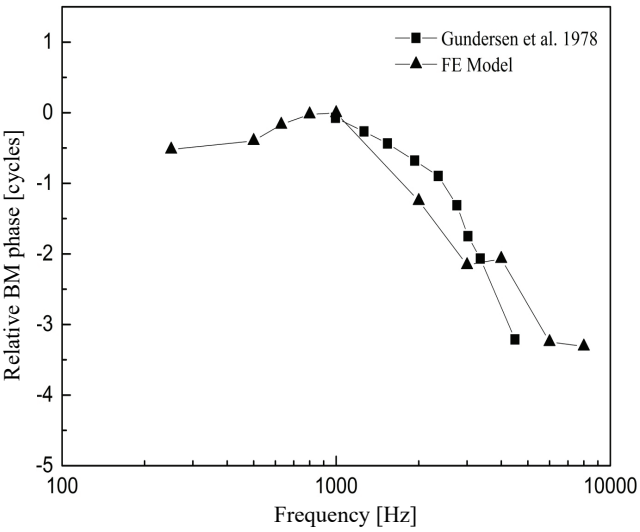

Fig. 3b. Phase of BM motion relative to stapes footplate motion for the human cochlea at 12 mm from the stapes

The cochlear input impedance reflects the acoustic resistance between the middle ear and the cochlea. Figure 4 shows that the cochlear impedance of the model-calculated is consistent with the experimental values obtained by Puria et al. [22] and Aibara et al. [1]. Besides, the trend of the predicted curve complies well with Puria et al.'s report.

Above three sets of comparisons demonstrate that the human ear sound transmission characteristics can be well reflected in our constructed human ear FE model. Thus, the middle ear disorder's influence on the RW stimulation can be studied based on this model.

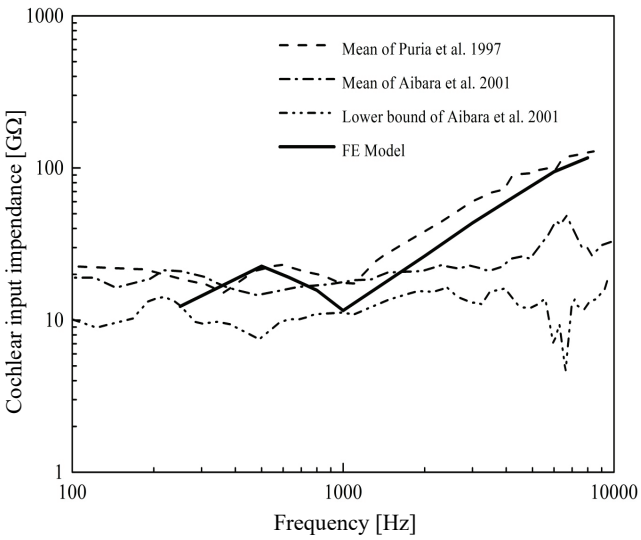

Fig. 4. Comparison of cochlear input impedance

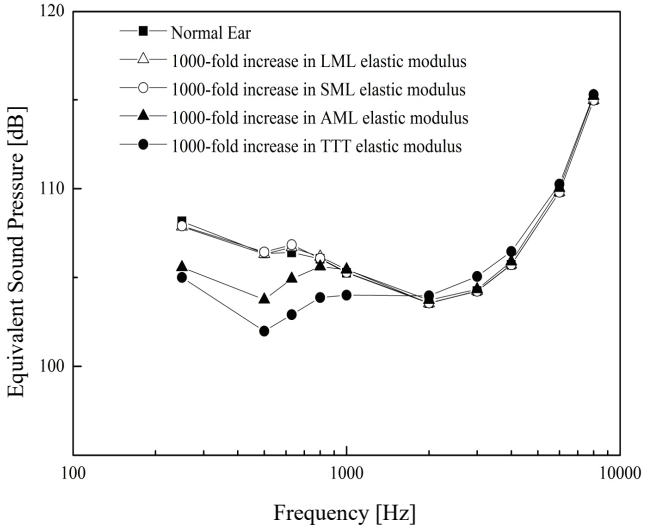

Fig. 5. The effect of the malleus fixation on RW stimulation

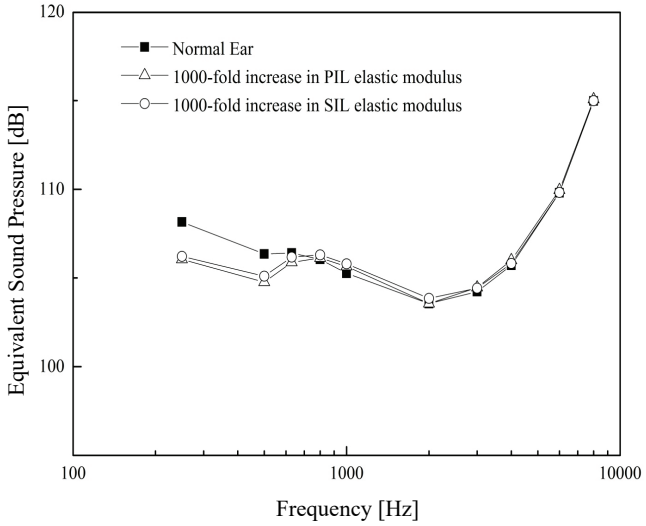

Fig. 6. The effect of the incus fixation on RW stimulation

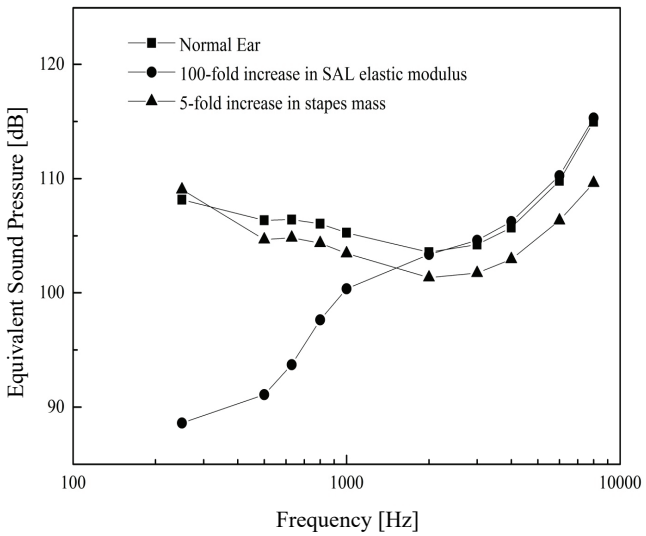

Fig. 7. The effect of the stapes fixation and abnormal growth on RW stimulation

3.2. Effect of the typical lesions in otosclerosis and otitis media on RW stimulation

3.2.1. Effect of the malleus fixation on RW stimulation

Figure 5 shows the model-predicted ESP curves of four types of malleus fixation under the 50 μN RW stimulation. The result of the normal ear was also compared with their results. It can be seen that the hardening of LML and SML have slight effect on RW stimulation. In contrast, the hardening of the AML and the TTT deteriorate the RW stimulation significantly at lower frequencies (AML: <1000 Hz, TTT: <2000 Hz); the corresponding maximum drop of their ESPs is 2.6 dB and 4.4 dB at 500 Hz, respectively.

3.2.2. Effect of the incus fixation on RW stimulation

The influences of two types of incus fixation on RW stimulation are shown in Fig. 6. Likewise, the hardening of PIL and SIL mainly affect the RW stimulation performance at lower frequency (<800 Hz), with a maximum decrease of 2.1 dB and 1.9 dB at 250 Hz, respectively. They have a little impact on the RW stimulation's ESP at mid-high frequencies.

3.2.3. Effect of the stapes fixation and abnormal growth on RW stimulation

The influences of stapes fixation and stapes abnormal growth on RW stimulation performance are shown in Fig. 7. It can be seen that the stapes abnormal bone growth, which was simulated by increasing the stapes mass 5-fold, has little effect on RW stimulation's lower-frequency performance (<500 Hz). Whereas, the ESP starts to drop along with the increase of the frequency, and the maximum amount of deterioration on ESP is about 5.4 dB at 8000 Hz. The hardening of the SAL slightly affects the ESP of RW stimulation at higher frequencies (above 2000 Hz), but deteriorates the RW stimulation performance prominently at lower frequency, the maximum deterioration is 19.5 dB at 250 Hz.

3.2.4. Effect of RWM lesions in otitis media on RW stimulation

Figure 8 shows the RW stimulation's ESP curves with RWM lesions. It indicates that the change of the

RWM's thickness in SOM has smaller influence on RW stimulation's ESP than on the others, the maximum decrease is 2.4 dB at 250 Hz. However, with the OM getting worse, it enlarges the effect on the RW stimulation especially at the low frequency (<800 Hz). Specifically, for the POM and COM, they deteriorate the low-frequency ESP of the RW stimulation, with a maximum decrease of 3.3 dB and 5.5 dB at 250 Hz, respectively. In terms of the AOM, it will boost the RW stimulation's low-frequency response when the elastic modulus change of the RWM is also considered, the maximum increase is 1.4 dB at 250 Hz. Moreover, the AOM reduces the RW stimulation's mid-frequency response slightly, the maximum deterioration is 1 dB at 600 Hz.

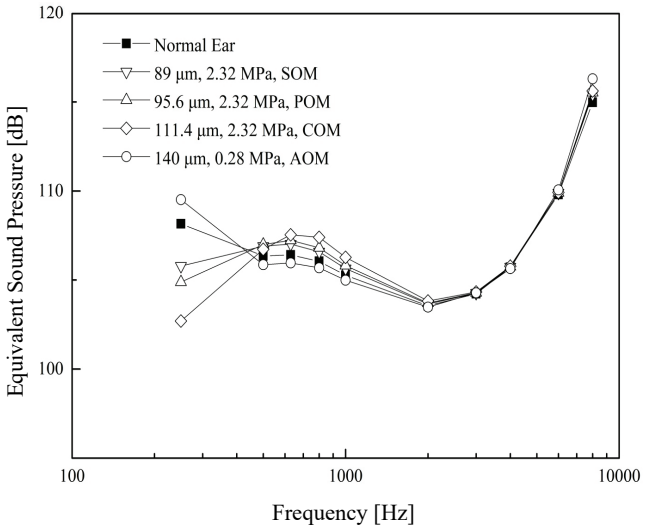

Fig. 8. The effect of the RWM lesions in OM on RW stimulation

4. Discussion

Due to the complex geometry and ultrastructural characteristic of the human ear, systematical experimental research on RW stimulation based on human ear temporal bone is difficult to conduct. Considering the finite element method has the advantage for simulating the complex biological system, many researchers have used this method to study human ear sound transmission mechanism [9], [10], [26] and assist the design of middle ear implant [17], [28]. Thus, in this paper, we also established a human ear FE model including the middle ear and the cochlea to aid our study. Since the cavity of the middle ear has a small impedance on the ear movement, it does not appear in this model [30]. Besides, the cochlea was simplified as a straight tube rather than a spiral structure. The cochlear spiral structure mainly improves the sound spreading at lower frequencies [19], whereas the sensorineural hearing loss concerned by MEIs mainly occurs at high frequency. Thus, this model simplification on the cochlea also has little effect on our study.

In the process of RW stimulation, RW and ossicular chain connecting to the oval window can be regarded as resistance to the energy transmission. Therefore, the RW stimulation's performance will be weakened when their impedance increases. In terms of the effect of the otosclerosis, our results show that the hardening of all the ligaments and tendons mainly deteriorate the RW stimulation performance at lower frequencies, which can be explained by the fact that the stiffness impedes the motion at low frequencies in dynamic system. However, the degree of these deteriorations is different among different ossicles' fixations, the hardening of the SAL that induces the stapes fixation has a much more significant influence than the other ligaments' hardening associated with the fixation of the malleus or incus. This may attribute to the lower elastic modulus of the incudostapedial joint, which decreases the influence of the movement of the malleus and incus on the RW stimulation. In contrast to the influence of these ligaments' hardening, the stapedial abnormal bone growth reduces the performance of the RW stimulation significantly at higher frequencies. This result may be caused by a fact that adding the mass shifts the resonance of whole system toward the lower frequencies.

Along with the increase of the thickness of the RWM caused by the OM, the RW stimulation's low-frequency performance is declined. This trend is comply with Yao et al.'s report [27]. In contrast, for the AOM, in which the RWM's elastic modulus decrease at the same time, its effect on the RW stimulation will be different. Specifically, the AOM increase the RW stimulation's low-frequency performance slightly.

The above results prove that the middle ear disorder's impact on the RW stimulation is considerable, especially the stapes' fixation in otosclerosis, the 19.5 dB deterioration is large enough compared to the RW stimulation's outcomes (30 dB) reported in clinical studies. Besides, different types of middle ear disorders have different influences. The hardening of the studied tissues and the thickening of the RWM mainly deteriorated the lower-frequency performance of the RW stimulation, while the stapedial abnormal bone growth severely affected the performance at high frequency. Thus, the effects of the middle ear disorder need to be considered during the design of the actuator for RW stimulation to reduce the postoperative

variability of the RW stimulation. The results of this paper not only provide references for the follow-up researches, but also provide supports for clinical applications of RW stimulation type MEIs.

Low-frequency band, especially below 100 Hz, is very important for the perception of music quality in the human ear, and the sensitivity of the human ear to these low-frequency sounds is strengthened by the spiral structure of the cochlea significantly. Specifically, the spiral cochlea redistributes the incoming wave energy toward the wall, especially along its innermost, tightest, apical turn [19], and this part is sensitive to low frequency. Therefore, for the analysis of the low frequency below 100 Hz, establishing a spiral cochlea is the best choice. Currently, a few upmarket hearing aids have a wider working frequency band, while most hearing aids work at a frequency range of 250–4000 Hz. In order to provide a more complete reference for the design of RW stimulation type MEIs, especially those considering the low-frequency function, a spiral cochlear model needs to be established in the next step. In addition, not only the pathology of the disorders is diverse, but also its combination form in clinical is variable, so more disorders and its combination treated with RW stimulation type MEIs will be analyzed in the future.

It should be mentioned that one limitation of our current study is that the modeling is just based on one human temporal bone. The anatomical differences of the human ear can induce individual variation in our results. To investigate the influence of human ear geometries' variation on FE model-predicted results, Daniel et al. [11] established three human ear FE models based on the scans of different human temporal bones, and compared the model-calculated stapes responses with the same modeling definitions and parameters. They found that the geometrical variation only induce quantitative differences of 4 dB in the lower frequencies and up to 6 dB around 2 kHz, but similar shapes in the calculated response curves. Thus, the patients' individual geometrical differences may alter our results quantitatively at lower frequencies and frequencies around 2 kHz. Nevertheless, the overall trend of our results still holds under different individual middle ear geometries.

5. Conclusion

To reduce the variability of the postoperative performance of the RW stimulation, the influence of typical middle ear disorders in otosclerosis and otitis media on the RW stimulation has been comparatively investigated. To aid this analysis, a human ear FE model based a serial of Micro-CT scanning images was constructed and verified. Our results show that, in the otosclerosis, the RW stimulation's ESP was severely deteriorated due to the stapedial abnormal bone growth at higher frequencies, while the hardening of ligaments and tendons prominently decreased the RW stimulation at lower frequencies. Besides, among hardening of the studied tissues, the influence of the SAL's hardening was much more significant. For the OM, the thickening of the RWM mainly decreased the RW stimulation's performance at lower frequencies. Whereas, when the elastic modulus' reduction of the RWM was considered at the same time for the AOM, it boosted the lower-frequency performance of the RW stimulation. The influence of the middle ear disorder on the RW stimulation is considerable and variable, and should be considered during the design of the RW stimulation type MEIs.

Acknowledgements

This research was funded by the Fundamental Research Funds for the Central Universities (2017QNA19) and the Top-notch Academic Programs Project of Jiangsu Higher Education Institutions (PPZY2015B120).

References

[1] AIBARA R., WELSH J.T., PURIA S., GOODE R.L., *Human middle-ear sound transfer function and cochlear input impedance*, Hear Res., 2001, 152(1–2), 100–109.

[2] ARNOLD A., CCANDREIA S., *Factors improving the vibration transfer of the floating mass transducer at the round window*, Otol. Neurotol., 2010, 31(1), 122–128.

[3] BARROSO E., MA Z., TAVARES J.M.R., GENTIL F., *Computational algorithms for the segmentation of the human ear*, VipIMAGE 2011 – III ECCOMAS Thematic Conference on Computational Vision and Medical Image Processing, Real Marina Hotel & Spa, Olhão, Algarve, Portugal, 12–14 October 2011, 377–382.

[4] BEKESY G.V., *Experiments in hearing*, McGraw-Hill, New York 1960.

[5] BELTRAME A.M., MARTINI A., PROSSER S., GIARBINI N., STREITBERGER C., *Coupling the vibrant soundbridge to cochlea round window: Auditory results in patients with mixed hearing loss*, Otol. Neurotol., 2009, 30(2), 194–201.

[6] FERREIRA A., GENTIL F., TAVARES J.M.R., *Segmentation algorithms for ear image data towards biomechanical studies*, Comput. Method Biomec., 2014, 17(8), 888–904.

[7] FROST H., *Observations on the fundamental nature of otosclerosis*, [in:] H. Schuknecht (ed.)*Otosclerosis*, Little, Brown and Company, Boston, 1962.

[8] GAN R.Z., SUN Q., FENG B., WOOD M.W., *Acoustic-structural coupled finite element analysis for sound transmission in human ear--pressure distributions*, Med. Eng. Phys., 2006, 28(5), 395–404.

[9] GENTIL F., PARENTE M., MARTINS P., GARBE C., JORGE R.N., FERREIRA A., TAVARES J.M., *The influence of the mechanical behaviour of the middle ear ligaments: A finite element analysis*, P. I. Mech. Eng. C.-J. Mec., 2011, 225(1), 68–76.

[10] GENTIL F., PARENTE M., MARTINS P., GARBE C., PA O.J., FERREIRA A.J., TAVARES J.M.R., JORGE R.N., *The influence of muscles activation on the dynamical behaviour of the tympano-ossicular system of the middle ear*, Comput. Method. Biomec., 2013, 16(4), 392–402.

[11] GREEF D.D., PIRES F., DIRCKX J.J.J., *Effects of model definitions and parameter values in finite element modeling of human middle ear mechanics*, Hear Res., 2016, 344, 195–206.

[12] GUNDERSEN T., SKARSTEIN O., SIKKELAND T., *A study of the vibration of the basilar membrane in human temporal bone preparations by the use of the mossbauer effect*, Acta Oto-Laryngologica, 2009, 86(3–4), 225–232.

[13] HUBER A., KOIKE T., WADA H., NANDAPALAN V., FISCH U., *Fixation of the anterior mallear ligament: Diagnosis and consequences for hearing results in stapes surgery*, Ann. Otol. Rhinol. Laryngol., 2003, 112(4), 348–355.

[14] KOKA K., HOLLAND N.J., LUPO J.E., JENKINS H.A., TOLLIN D.J., *Electrocochleographic and mechanical assessment of round window stimulation with an active middle ear prosthesis*, Hear Res., 2010, 263(1), 128–137.

[15] KRINGLEBOTN M., GUNDERSEN T., KROKSTAD A., SKARSTEIN O., *Noise-induced hearing losses. Can they be explained by basilar membrane movement?*, Acta Otolaryngol. Suppl., 1979, 360 (Suppl. 360), 98–101.

[16] LIU H., CHENG J., YANG J., RAO Z., CHENG G., YANG S., HUANG X., WANG M., *Concept and evaluation of a new piezoelectric transducer for an implantable middle ear hearing device*, Sensors, 2017, 17(11), 2515.

[17] LIU H., XU D., YANG J., YANG S., CHENG G., HUANG X., *Analysis of the influence of the transducer and its coupling layer on round window stimulation*, Acta Bioeng. Biomech., 2017, 19(2), 103–111.

[18] MAIER H., SALCHER R., SCHWAB B., LENARZ T., *The effect of static force on round window stimulation with the direct acoustic cochlea stimulator*, Hear Res., 2013, 301(7), 115–124.

[19] MANOUSSAKI D., DIMITRIADIS E.K., CHADWICK R.S., *Cochlea's graded curvature effect on low frequency waves*, Phys. Rev. Lett., 2006, 96(8), 088701.

[20] MILLER M.H., SCHEIN J.D., *Selected complex auditory disorders*, J. Rehabil. Res. Dev., 2005, 42(4 Suppl. 2), 1–8.

[21] NAKAJIMA H.H., RAVICZ M.E., ROSOWSKI J.J., PEAKE W.T., MERCHANT S.N., *Experimental and clinical studies of malleus fixation*, The Laryngoscope, 2005, 115(1), 147–154.

[22] PURIA S., PEAKE W.T., ROSOWSKI J.J., *Sound-pressure measurements in the cochlear vestibule of human-cadaver ears*, J. Acoust. Soc. Am., 1997, 101(1), 2754–2770.

[23] RONG Z., GAN D.N., XIANGMING ZHANG, *Dynamic properties of round window membrane in guinea pig otitis media model measured with electromagnetic stimulation*, Hear Res., 2013, 301(1), 125–136.

[24] SAHNI R.S., PAPARELLA M.M., SCHACHERN P.A., GOYCOOLEA M.V., LE C.T., *Thickness of the human round window membrane in different forms of otitis media*, Arch. Otolaryngol. Head Neck Surg., 1987, 113(6), 630–634.

[25] TIAN J., HUANG X., RAO Z., TA N., XU L., *Finite element analysis of the effect of actuator coupling conditions on round window stimulation*, J. Mech. Med. Biol., 2015, 15(4), 1550048.

[26] WANG X., WANG L., ZHOU J., HU Y., *Finite element modelling of human auditory periphery including a feed-forward amplification of the cochlea*, Comput. Method Biomec., 2014, 17(10), 1096–1107.

[27] YAO W., TANG D., CHEN Y., LI B., *Study on vibration characteristics and transmission performance of round window membrane under inverse excitation*, J. Mech. Med. Biol., 2018, 1850033.

[28] ZHANG X., GAN R.Z., *A comprehensive model of human ear for analysis of implantable hearing devices*, IEEE T. Bio-Med. Eng., 2011, 58(10), 3024–3027.

[29] ZHANG X., GAN R.Z., *Dynamic properties of human round window membrane in auditory frequencies running head: Dynamic properties of round window membrane*, Med. Eng. Phys., 2013, 35(3), 310–318.

[30] ZWISLOCKI J., *Analysis of the middle-ear function*. Part I: *Input impedance*, J. Acoust. Soc. Am., 1962, 34(9B), 1514–1523.